The 2010 IEEE/RSJ International Conference on
Intelligent Robots and Systems
October 18-22, 2010, Taipei, Taiwan

Proposition and Development of a Robot Manipulator for Humanitarian Demining

Jayamuni Dinesh Anton Lakmal Silva, *Member, IEEE*

***Abstract*— This paper presents the proposition and development of a robot manipulator for demining. The manipulator concept is based on the demining method called "mine raking". The main objective is to safely excavate anti personal mines without being exploded while retaining sufficient force for excavation. The desired excavation force and the actual external force are compared and the error is converted in to a position deviation of the desired position trajectory, causing the manipulator end effector to move towards a safer excavation force. The kinetic and kinematic analyses are presented for the manipulator assuming quasi-static motion. Simulation results are presented for a time varying 2D external force vector.**

***Keywords*:** *Humanitarian demining, excavation, Impedance control,*

I. Introduction

THROUGOUT the world many countries including Sri Lanka has been severely affected by Anti Personal Mines (APM) and their effects [1]. Existence of APMs has become a huge obstacle for post – conflict civilian resettlement. Several organizations have been involved with this process but with estimated completion times in the order of decades. The need of a Humanitarian Demining (HD) solution is essential, that accelerates the process of HD with acceptable safety and quality measures.

Currently HD more relies on conventional tools and direct human involvement. Several fatal accidents happened so far while demining, and main key causes identified are insufficient training, mine excavation without proper force control, poor mine detection techniques. Details of accidents due to each cause are available in [2]. According to [2], mine excavation has been identified as the main cause of demining accidents acquiring 42% of all types.

Although demining machines have been developed in several forms, many of those are not suitable for the targeted operational environments, the Sri Lankan mine fields, because they do not meet the clearance requirement request by the UN (99.7% clearance). Most of these APM affected areas are densely populated so not enough space for a huge machine to maneuver. Many of these machines [3], [4] remove or disturbs the uppermost soil layer, (only 0.15m thick in many Sri Lankan mine fields), and the best portion for agricultural purposes. Therefore mass scale demining vehicles are not ideally suitable for these Sri Lankan mine fields.

These unique requirements demand an innovative solution for demining operations in Sri Lanka. The proposed demining robot must be capable of maneuvering through densely built up areas, thick vegetation, and inclined surfaces. Also it must identify suspected mine locations quickly and accurately. A manipulator should be available to excavate mine locations and to recover mines' exerting a safe force. Development of excavation manipulator is the major focus of this research paper. Another manipulator should be available with this demining robot capable of relocating the mine at a safer place to detonate later. Also the robot must be capable of withstand accidental mine explosions with easily recoverable damages.

There are several mobile robot platforms developed that maneuver through rough terrains either fully automated or remotely operated. A few of these are even commercially available. Therefore this research effort does not intend to do in depth study on developing a mobile robot platform for maneuvering.

Accurate mine detection is a challenge, because still there are no real "Mine Detectors" yet available. Many are "metal detectors" that only indicate existence of metal fragments of a mine. Innovative detection techniques [5], [6] have made progress specifically on how to distinguish a mine from other metal debris. For this project a standard metal detector is proposed for identifying suspected mine locations. The mine category that makes most harm for humans are APMs. This paper focuses demining of APMs only.

From Chapter II to Chapter IV an overview of existing APM clearance methods, research problem identification and the selection of targeted geographic area is presented. Chapter V describes related research done on demining robot manipulators. Chapters VI and VII describe conceptual design and mathematical modeling of manipulator. Chapter VIII to X explains the mine excavation procedure and its simulation and simulation results respectively. Limitations of simulation are presented in chapter XI. Chapter XII explains proposed future work.

II. Mine Raking

The robot manipulator concept was inspired by the demining method called "Mine Raking' (MR). Here demining operations begin first scanning the mine field with a metal

Manuscript received March 9, 2010. This work was self supported by J. D. A. L. Silva. Initial part of this research was funded by Sri Lanka National Science foundation under the grant RG/2004/E/02

J. D. A. L. Silva was with University of Moratuwa, Moratuwa, Sri Lanka. He is now with the OREL Solutions (Pvt) Ltd, No 49, Sri Jinarathana Road, Colombo 02, Sri Lanka.(e-mail: jayamuni@ieee.org).

detector. After marking the Suspected Mine Locations (SMLs) excavation starts targeting only SMLs. During MR the SMLs' upper ground surface is scraped by a rake, much similar to gardening, until a suspected object is found. The "object" may not necessarily be an APM. Many of these objects are metal fragments of exploded mines and bullets. Regardless of the object being buried equal attention is paid for each detector signal. This causes too many unnecessary excavations causing wastage of productive time, labor and funds.

MR is not the best demining method compared to manual demining using a shovel and prodder. Still MR preserves unique joint movements that a robot can imitate very easily with minimal degrees of freedom. Using shovel and prodder is much safer for human deminers but its associated multidimensional joint movements make it more difficult for a robot to imitate.

III. Research Problem Identification

Currently MR is done manually without force control. The risk and difficulty of this operation is if the excavation force exceeds a threshold value typically 70N above a mine, it may explode. If sufficient force not exerted excavation becomes impossible. International Mine Action Standard (IMAS) requires a minimum mine excavation depth of 130mm [7]. Deminers reach this level by gradually increasing excavation depth step by step starting from ground surface. The major challenge in demining is to exert a sufficient force for excavation, while retaining it below threshold value and to progressively excavate the soil till the required depth reached for inspection.

If a robot manipulator used to perform such a task, ideally its controller should be capable of exerting a desired force profile, while tracking a desired excavation position trajectory. But fundamentally it is impossible to control both position and force to the same degree of freedom [8]. This is because interaction force between manipulator and contact surface depends only on the mechanical impedances of both end effector and contact surface. For mine excavation, out of two key control parameters, force is considered to be more critical than position. A control algorithm is developed such that the manipulator attempts to exert a desired force profile while tracking a desired position trajectory. When manipulator fails to retain desired force it will result a position trajectory deviation causing a reduction of interaction force.

IV. Targeted Operational Environment

The robot to be expected operating on mine fields in the North and Eastern Provinces of Sri Lanka. Many of these areas soil is composed of higher sand content loosely bonded granules and a limestone layer beneath 0.15m depth from the surface. During excavation impact type loads at rake tip rarely occur. APMs are buried at the ground surface level. Many of these areas are densely populated and with medium size houses.

V. Related Work

In the first paper [9] of this research programme, a similar manipulator configuration was proposed but with a completely different control strategy. Earlier the external environmental force was estimated using soil impedance. The interaction force between environment and rake tip was determined using a time lag of the actual position trajectory. The major drawback was soil impedance vary from location to location also with environmental condition, requiring continuous parameter adjustments while operation.

A master slave type demining hand been proposed by Naota [10] imitating common demining operation using shovel and prodder. This is entirely mechanically operated and claimed to be suitable for remote areas. A weight compensated pantograph manipulator has been proposed by Tojo et al. [11].

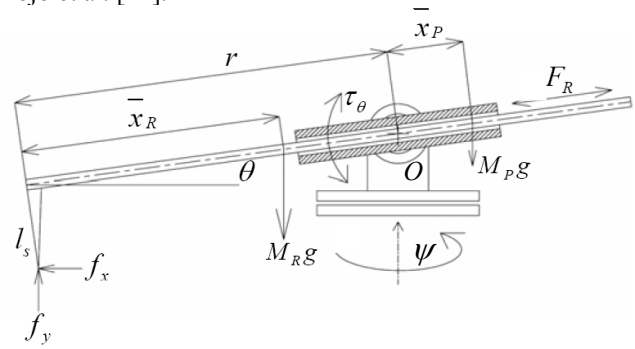

Fig. 1. Robot Manipulator Conventional Diagram

VI. Robot Manipulator Development

A. Manipulator Workspace

In Fig.1, the proposed manipulator's conventional diagram is shown. The manipulator consists of a sliding joint, with a stroke length r_{max} , and it is mounted on a rotary joint that can rotate around a horizontal axis with an angular stroke θ_{max}. This subassembly is mounted on another rotary joint that can rotate around a vertical axis with an angular stroke ψ_{max}. A mine excavation rake used by the Sri Lanka Army Humanitarian Demining Unit, will be mounted at the end of sliding joint making rake tips the end effector. These rakes are solely design for APM excavation. By suitably varying θ and r the end effector can be traversed along a vertical planar surface tracing a desired trajectory $\underline{\boldsymbol{x}}_d$. A complete mine excavation task can be done by varying θ and r alone assuming the rake has sufficient width. Once a mine location identified ψ can be fixed. Therefore for this research only the variation of r, θ and forces along the vertical plane considered.

B. Manipulator Design

A load cell, measures the axial force F_R along the rake, while a torque sensor measures load torque τ_θ around the pivot 'O'. The torque sensor can be located at the rake end thus simplifying analysis but here it is located at the pivot to facilitate further developments. The sliding joint comprise of a linear positioning device operated by a belt drive coupled to the rake motor, a geared type. The horizontal axis rotary

joint too is operated by a geared motor identical to the rake motor.

The manipulator will be designed to withstand accidental mine explosions with minimal harm. No sensor located near the end effector. Even at an explosion the damage is much less because only the rake, comparably very cheap may get damaged.

C. Proposed Field Operation

The manipulator does mine field excavation in a semi – automated mode. The integrated robot platform will maneuver through mine field under the guidance of a human operator remotely located. Guiding the robot platform towards a mine location and defining the mine location too will be done by the human operator. Identification of mine location and its position coordinates will be identified with standard mine detectors and positioning devices such as GPS. The complete excavation operation is done by the manipulator automatically once commanded.

VII. Mathematical Model Development

The robot consists of a three degrees of freedom manipulator with one sliding joint and two rotary joints. The workspace is limited by sliding joint stroke length and rotary joints' maximum angular displacements. The manipulator will be designed to have very slow linear and rotary speeds and their time derivatives. As a result inertial loads become comparably negligible. A force sensor is available to measure axial force F_R along the rake. A torque sensor is available to measure load torque $\boldsymbol{\tau_\theta}$ around pivot 'O'. Both measurements are assumed to be pre-processed and electrical noise free. During excavation rake tip is affected by a resultant external force. Orthogonal components of this force are included in equation (1) in vector form,

$$\underline{f}_e = \begin{pmatrix} -f_x & f_y \end{pmatrix}^T \tag{1}$$

For analysis purposes origin for both polar and cartesian coordinate systems, located at center of pivot 'O'. Polar to cartesian mapping is defined in equation (2),

$$\underline{X} = \begin{pmatrix} x & y \end{pmatrix}^T = \begin{pmatrix} -(r\cos\theta - l_s \sin\theta) & -(r\sin\theta + l_s \cos\theta) \end{pmatrix}^T \tag{2}$$

Mapping of external force vector into manipulator internal disturbance load vector done by the jacobian matrix shown in equation (3),

$$\underline{J}^T(r,\theta) = \begin{pmatrix} -\cos\theta & -\sin\theta \\ (r\sin\theta + l_s\cos\theta) & -(r\cos\theta - l_s\sin\theta) \end{pmatrix} \tag{3}$$

Manipulator internal disturbance load $\boldsymbol{\underline{F}_{dis}}$, vector is defined in equation (4),

$$F_{dis} = \begin{pmatrix} F_R \\ \tau_\theta - (r - \bar{x}_R) M_R g \cos\theta + M_P \bar{x}_P \cos\theta \end{pmatrix} \tag{4}$$

Here 'M' and '$\bar{x}$' refer to mass and location of center of gravity respectively. Throughout the analysis the subscript "R" refers the sliding joint, the Rake while "P" refers rotary joint, the Platform.

By applying Newton's second law, along the direction of $\hat{r}$, and considering force moments around 'O' the set of equations relating the external environmental forces to the measurable forces and torques is written in vector matrix form as shown in equation (5).

$$\begin{pmatrix} -\cos\theta & -\sin\theta \\ (r\sin\theta + l_s\cos\theta) & -(r\cos\theta - l_s\sin\theta) \end{pmatrix} \begin{pmatrix} -f_x \\ f_y \end{pmatrix} = \begin{pmatrix} F_R \\ \tau_\theta - (r - \bar{x}_R) M_R g\cos\theta + M_P \bar{x}_P \cos\theta \end{pmatrix} \tag{5}$$

In compact form the above system of equations can be written as defined in equation (6).

$$\underline{J}^T(r,\theta)\underline{f}_e(x,y) = \underline{F}_{dis} \tag{6}$$

As all the elements of and $\underline{J}(r,\theta)$ and $\underline{F}_{dis}$ are known as either previous estimates or sensor measurements, the actual external force vector as defined in equation (7), can be calculated by,

$$\underline{f}_e = [\underline{J}(r,\theta)^T]^{-1} \underline{F}_{dis} \tag{7}$$

Where, in equation (8) $[\underline{J}(r,\theta)^T]^{-1}$ is defined as,

$$[\underline{J}(r,\theta)^T]^{-1} = \frac{1}{r}\begin{pmatrix} -(r\sin\theta - l_s\cos\theta) & -(r\cos\theta - l_s\sin\theta) \\ \sin\theta & -\cos\theta \end{pmatrix} \tag{8}$$

The actual external forces are then compared with the desired force vector, $\underline{f}_d$ defined in equation (9),

$$\underline{f}_D = \begin{pmatrix} -f_{Dx} & f_{Dy} \end{pmatrix}^T \tag{9}$$

The force deviation is transformed in to a position deviation $\boldsymbol{\underline{X}_E}$ defined in equation (10) for time domain by a predefined manipulator impedance parameter matrix $\boldsymbol{\underline{K}_{imp}}$ defined in equation (11). Here 'M', 'B' and 'K' refer mass, viscous and stiffness effects of manipulator as seen from a mechanical impedance perspective. Numerical values of these parameters will define the dynamic behavior of manipulator such as an under damped, over damped or an oscillatory system. Subscripts '$_{DX}$' and '$_{DY}$' refers the desired values in horizontal and vertical directions respectively.

$$\underline{X}_E(t) = \begin{pmatrix} x_E & y_E \end{pmatrix}^T = \underline{K}^{-1}{}_{imp}(t)(f_D - f_e) \tag{10}$$

$$\underline{K}_{imp}(s) = \begin{pmatrix} \frac{1}{M_{DX}s^2 + B_D s + K_{DX}} & 0 \\ 0 & \frac{1}{M_{DY}s^2 + B_{DY}s + K_{DY}} \end{pmatrix} \tag{11}$$

$\boldsymbol{\underline{X}_E}$ then subtracted from the desired position vector $\boldsymbol{\underline{X}_D}$ defined in equation (121), as a corrective component. The resultant called commanded position vector $\boldsymbol{\underline{X}_C}$ as defined in equation (13). This is in cartesian form and be transformed into a polar form vector $\boldsymbol{\underline{\theta}_{CM}}$, as defined in the equation (14).

$$\underline{X}_D = \begin{pmatrix} x_D & y_D \end{pmatrix}^T \tag{12}$$

$$\underline{X}_C = \begin{pmatrix} x_C & y_C \end{pmatrix}^T = \begin{pmatrix} x_D - x_E & y_D - y_E \end{pmatrix}^T \tag{13}$$

$$\underline{\theta}_{CM} = \begin{pmatrix} r_C \\ \theta_C \end{pmatrix} = \begin{pmatrix} \left| \sqrt{(x_C{}^2 + y_C{}^2 - l_s{}^2)} \right| \\ Tan^{-1}\left\{ \frac{(y_C r_C - l_s x_C)}{(x_C r_C + l_s y_C)} \right\} \end{pmatrix} \tag{14}$$

Respectively r_c and $\underline{\theta}_C$ are the commanded position trajectories for the sliding and rotary joints. $\boldsymbol{\underline{\theta}_{CM}}$ is compared with the actual position trajectory $\boldsymbol{\underline{\theta}_{AC}}$ defined in equation (15).

$$\underline{\theta}_{AC} = \begin{pmatrix} r_A & \theta_A \end{pmatrix}^T \tag{15}$$

The resultant is the compensated position vector $\underline{\boldsymbol{\theta}}_{\boldsymbol{CMP}}$ defined in equation (16).

$$\underline{\theta}_{CMP}=\begin{pmatrix} r_{CM} & \theta_{CM} \end{pmatrix}^T=\begin{pmatrix} r_C-r_A & \theta_C-\theta_A \end{pmatrix}^T \tag{16}$$

Actually $\underline{\boldsymbol{\theta}}_{\boldsymbol{CMP}}$ is the error resulting from standard feedback loop. $\underline{\boldsymbol{\theta}}_{\boldsymbol{CMP}}$ is passed through a PID controller of which defined in matrix form in equation (17) with parameters in usual notation.

$$\underline{H}(s)=\begin{pmatrix} K_{PR}+\dfrac{K_{IR}}{s}+K_{DR}s & 0 \\ 0 & K_{PP}+\dfrac{K_{IP}}{s}+K_{DP}s \end{pmatrix} \tag{17}$$

Outputs from the controllers are fed into DC Brushed motors' drivers. For simulations motor driver assumed to be of fast dynamics compared to other mechanical and electrical components and considered to be constant gain type until reaches maximum motor input voltage 24V while, beyond 24V the output is saturated. Motor drivers parameters are defined in equation (18).

$$\underline{M}(s)=\begin{pmatrix} M_R(s) & 0 \\ 0 & M_P(s) \end{pmatrix} \tag{18}$$

Output of motor drivers is the voltage supply vector $\underline{\boldsymbol{V}}_{\boldsymbol{S}}$ to the motors defined in equation (19). The back electro motive force voltage vector $\underline{\boldsymbol{V}}_{\boldsymbol{B}}$ defined in equation (20) while Motor velocity coefficients are included in matrix $\underline{\boldsymbol{K}}_{\boldsymbol{VB}}$, defined in equation (21). Here $\dot{\theta}_R$ and $\dot{\theta}_P$ are rake and platform motor angular speeds respectively.

$\underline{\boldsymbol{V}}_{\boldsymbol{B}}$ is subtracted from $\underline{\boldsymbol{V}}_{\boldsymbol{S}}$ before feeding into motor electrical parameter matrix $\underline{M}_E$ is defined in equation (22). Here the parameters '*L*', '*R*', '*K*' refer to motor armature inductance, resistance and torque constant respectively.

$$\underline{V}_S=\begin{pmatrix} V_R & V_P \end{pmatrix}^T \tag{19}$$

$$\underline{V}_B=\begin{pmatrix} V_{BR} & V_{BP} \end{pmatrix}^T=\underline{K}_{VB}\begin{pmatrix} \dot{\theta}_R & \dot{\theta}_P \end{pmatrix}^T \tag{20}$$

$$\underline{K}_{VB}=\begin{pmatrix} K_{VR} & 0 \\ 0 & K_{VP} \end{pmatrix} \tag{21}$$

$$\underline{M}_E(s)=\begin{pmatrix} \dfrac{K_{TR}}{(L_R s+R_R)} & 0 \\ 0 & \dfrac{K_{TP}}{(L_P s+R_P)} \end{pmatrix} \tag{22}$$

Output from $\underline{\boldsymbol{M}}_{\boldsymbol{E}}\boldsymbol{(s)}$ is the internally generated torque vector. This is disturbed by the disturbance load vector $\underline{\boldsymbol{F}}_{\boldsymbol{dis}}$ being scaled down by gear reduction $\boldsymbol{N_R}$. The rake axial force also transformed in to rake geared motor torque input F_R/a_R. a_R is the radius of major pulley driving the rake belt. The resultant torque output $\underline{\boldsymbol{\tau}}_{\boldsymbol{RES}}$ is defined in equation (23) as

$$\underline{\tau}_{RES}=\underline{\tau}_{INT}-\begin{pmatrix} F_R/a_R N_R \\ \{\tau_\theta-(r-\bar{x}_R)M_R g\cos\theta+M_P\bar{x}_P\cos\theta\}/N_R \end{pmatrix} \tag{23}$$

Resultant torque is fed into motor mechanical parameter matrix $\underline{\boldsymbol{M}}_{\boldsymbol{M}}\boldsymbol{(s)}$ defined in equation (24). The symbols *J* and *B* refer to inertia and viscous friction parameters. Subscript "*eq*" refers to the equivalent value for gear – motor assembly.

$$\underline{M}_M(s)=\begin{pmatrix} \dfrac{1}{(J_{eqR}s+B_{eqR})s} & 0 \\ 0 & \dfrac{1}{(J_{eqP}s+B_{eqP})s} \end{pmatrix} \tag{24}$$

Output from $\underline{\boldsymbol{M}}_{\boldsymbol{M}}\boldsymbol{(s)}$ is the actual position vector in polar form defined in equation (14). Actual position trajectory can be transformed in to cartesian form for results visualization through the following transformation defined in equation (25).

$$\underline{X}_A=\begin{pmatrix} x_A \\ y_A \end{pmatrix}=\begin{pmatrix} -(r_A\cos\theta_A-l_s\sin\theta_A) \\ -(r_A\sin\theta_A+l_s\cos\theta_A) \end{pmatrix} \tag{25}$$

The complete block diagram for the robot manipulator is shown in Fig.3. The inputs, out puts and disturbance force vectors and how they affect systems performance are shown here.

VIII. Mine Excavation

A. Mine Location Identification

A conventional mine detector to be used for suspected mine location identification. Based on the target location the excavation trajectory is set.

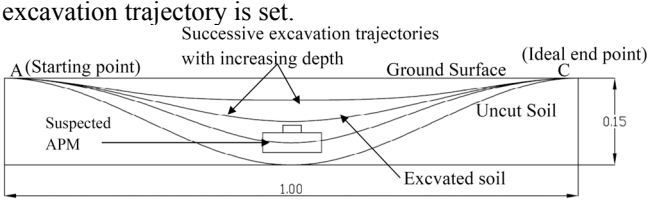

Fig. 2. Proposed APM Excavation Trajectory (all dimensions are in meters)

B. Excavation Profile

The soil excavation profile is defined by the excavation depth *'d'*, length of excavation '*l*' path and its width '*w*'. Here they are set to be 0.15m maximum, 1.00m and 0.20m respectively. A single mine excavation task consists of a collection of such trajectories with increasing depth up to 0.15m. For analysis purposes the profile is simplified to a two dimensional curve lying on a vertical plane. Each trajectory is approximated to a portion of a sinusoidal curve for ease of computation. This is shown in Fig.2. The equation (25) is defined as the equation of excavation shown below,

$$y=-\frac{d}{2}\{1-\cos(2x\pi)\} \tag{26}$$

Here *x* and *y* refer to horizontal and vertical position of excavation profile respectively.

C. Performing Mine Excavation

Excavation starts from the far end '*A*' tracking the desired position trajectory as far as the desired environmental force matches the external environmental force. If the external environmental force is different from the desired then actual trajectory is altered as permitted by the manipulator internal impedance parameters which transform force errors into position deviations. This type of trajectory deviation is acceptable because for such applications, as the key objective is to excavate the mine location safely rather than

following a position trajectory accurately. Ideally excavation trajectory should end from point 'C'. Depending on effects of external forces the actual end point may be different.

IX. Mine Excavation Simulation

It is assumed a suspected mine location is found and the excavation trajectory starting position is set already. Identifying a mine location and guiding the robot towards it, is out of scope of this research. Well developed techniques and machines are commercially available for similar applications. The manipulator then commanded to follow the position trajectory shown in Fig. 4 (a) from the starting point '*A*'. The desired force is set to be 50N continuous. If required the desired force vector could be set as time varying parameter.

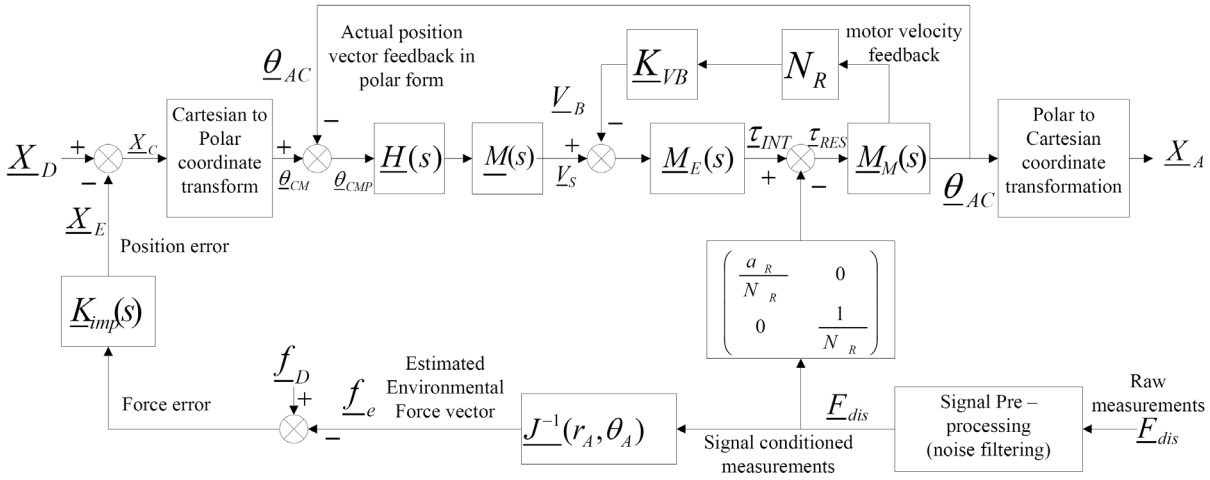

A. Fig. 3. Block Diagram Description of Manipulator

A complete demining operation consists of a few excavation trajectories, here simulation results are presented only for a single trajectory. The manipulator starts excavation following the desired trajectory. As long as the desired force and the actual environmental force are equal the system operates as a standard position controller with feedback.

It is assumed the inertial loads and forces are negligible compared to external environmental force and gravitational force components. As shown in Fig. 4(b) and (c), the manipulator is subjected to an incremental environmental force profiles starting from *50N*, with a peak value of *70N* vertically and *80N* horizontally and later slowly decaying up to *50N*. This type of force profiles occur in sandy loose – bonded soil. But the model is capable of exerting any time variant force profile. Here constant and linearly increasing force profiles are selected, due to quasi-static motion of end effector. Rapid increase of force is not expected. Detailed study on rapid force variations and analysis of the effects of manipulator inertial dynamics will be included in future work. To prevent over excavation in the case of a lower external force than the desired force the controller can be easily set to follow only the desired trajectory then. In this simulation only equal and higher external forces compared to the desired forces are considered.

X. Simulation Results

Simulation results are available in Fig. 4 (a), (b) and (c). The coordinates of vertical and horizontal positions are measured with reference to the origin located at the center of manipulator pivot 'O'.

Fig. 4(a) shows how the actual and desired position trajectories deviate in the presence of an above threshold forces as shown in figures 4 (b) and (c). As long as both the actual and desired forces are equal manipulator tracks the desired position trajectory. When the force rises beyond 50*N*, a trajectory deviation occurs. This is the result of transforming a force deviation in to a position deviation. The amount of deviation and the transient properties can be adjusted by suitably varying the manipulator impedance parameters defined in equation (10). The magnitude of impedance defines the 'softness' of the manipulator. For example if the manipulator stiffness becomes higher it will respond even for small force deviations causing a large position deviation. Then it will act more like a pure force controlled manipulator. If the stiffness becomes lower manipulator becomes insensitive to external force disturbances. By this way it will be more like a pure position controlled manipulator. Therefore in this manner APM excavation is possible without exerting an above threshold.

XI. Limitations of Simulations

Here the analysis was done assuming a quasi static motion with negligible inertial loads. Also this method only suitable for loosely bonded soil types where smooth force variations possible.

Here the external force profile is predefined. It will not dynamically get adjusted with the deviation of manipulator end effector. For example the actual input force profile selected for simulation rises up to *20N* beyond threshold. As a result the manipulator makes a deviation of trajectory but still the exerted force profile not gets adjusted just like in practice. Practically if the manipulator deviated due to a higher force, then the actual external force too should get

reduced due to the loosing of contact. This could be overcome by equivalently modeling soil surface to a mass spring damper system in future work.

XII. Future Work

The dynamic analysis will be done for rapid manipulator motions considering the properties of tightly bonded soil types. In addition implementation of controllers in real time will also be studied. A hardware prototype will be developed, to be field tested for different soil conditions under a controlled environment.

XIII. Conclusion

The conceptual development and performance is simulated for the demining robot. But simulation results might not identically representing the real world performance. Especially for these types of robots field tests are essential part of product development. Due to the dangers associated with these types of work simulations play an important role assisting systems design and performance evaluation.

XIV. Acknowledgement

The author thanks to Dr. Narendra de Silva and the Department of Mechanical Engineering, University of Moratuwa for the guidance and support.

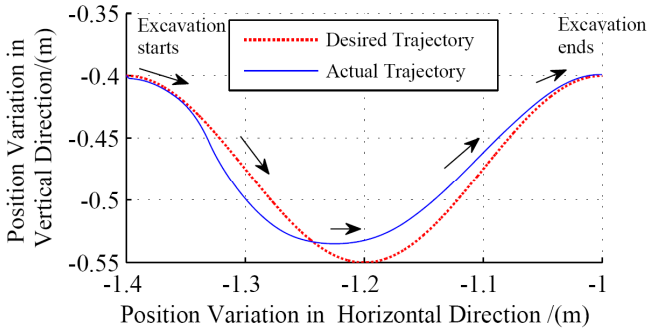

Fig. 4(a). Comparison of Desired and Actual Position Trajectories (arrows indicate the path of excavation)

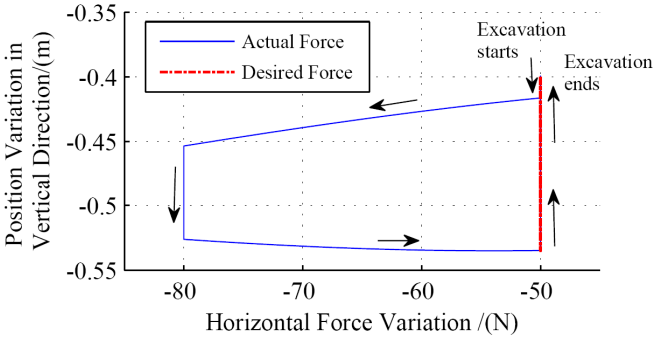

Fig. 4(b). Variation of Desired and Actual External Force along Horizontal direction (arrows indicate relationship with excavation path)

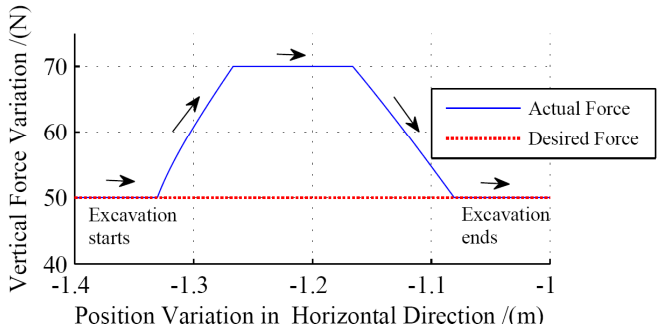

Fig. 4(c). Variation of Desired and Actual External Force along vertical direction (arrows indicate relationship with excavation path)

XV. References

[1] The Mine Action Information at James Madison University. Available: [online] http://maic.jmu.edu/

[2] "*The Record of Accidents in Humanitarian Demining*", Landmine Accidents Database ver 4, Available:[online] http://www.ddasonline.com/

[3] "Mechanical *Demining Equipment Catalogue 2006*", Geneva Center Humanitarian Demining 7bis, avenue de la Paix, P. O. Box 1300, CH – 1211 Geneva 1, Switzerland

[4] Christopher Wanner, "*Mixing It Up: The Rotary Mine Comb*", Journal of ERW and Mine Action, Issue 12.2, Winter 2008/2009

[5] R. K. L. Van Dam, B. Borchers, J. M. Hendricks, "*Strength of landmine signatures under different soil conditions: Implications for sensor fusion*", Journal of systems science vol 36 number 9, pp 573-588. Taylor & Francis

[6] Fernandez Manuel, Lewis Adam, Littman François, Technical Note 09.10/01 version 01, PROM 1 "Metal Detector Warning", Technical Notes For Mine Action. Available: http://www.hdic.jmu.edu

[7] "Clearance Requirements" International Mine Action Standard IMAS 09.10, Second Edition 01 Jan 2003, pp 2.

[8] N. Hogan, "*Impedance Control: An Approach to Manipulation: Part I–Theory"*, Journal of Dynamic Systems, Measurement, and Control, vol 107, March 1985, pp 1-7.

[9] Lakmal Silva, Thrishantha Nanayakkara, "*Impedance Control of a Robot Manipulator for Demining*", Proc. Of International Conference on Information and Automation 2005, pp 282-287.

[10] Naota Furihata, Shigeo Hirose, "Development of Mechanical Master-Slave Hand for Demining Operation", Proc. Of IEEE International Conference on Robotics and Automation 2004, pp 2017-2024.

[11] Yuki Tojo, Paulo Debenest, Edwardo F Fukushima, Shiego Hirose, "Robotic System for Humanitarian Demining, Development of Weight Compensated Pantograph Manipulator", Proc. Of IEEE International Conference on Robotics and Automation 2004, pp 2025 – 2030.